

Revisiting the quest for a universal log-law and the role of pressure gradient in “canonical” wall-bounded turbulent flows

Peter A. Monkewitz*

*Faculty of Engineering Science, Swiss Federal Institute of Technology (EPFL) CH-1015,
Lausanne, Switzerland*

(Received 23 February 2017; published 13 September 2017)

The trinity of so-called “canonical” wall-bounded turbulent flows, comprising the zero pressure gradient turbulent boundary layer, abbreviated ZPG TBL, turbulent pipe flow, and channel/duct flows has continued to receive intense attention as new and more reliable experimental data have become available. Nevertheless, the debate on whether the logarithmic part of the mean velocity profile, in particular the Kármán constant κ , is identical for these three canonical flows or flow-dependent is still ongoing. In this paper, the asymptotic matching requirement of equal κ in the logarithmic overlap layer, which links the inner and outer flow regions, and in the expression for the centerline/free-stream velocity is reiterated and shown to preclude a universal logarithmic overlap layer in the three canonical flows. However, the majority of pipe and channel flow studies at friction Reynolds numbers Re_τ below $\approx 10^4$ extract from near-wall profiles the same κ of 0.38–0.39 as in the ZPG TBL. This apparent contradiction is resolved by a careful reanalysis of high-quality mean velocity profiles in the Princeton “Superpipe” and other pipes, channels, and ducts, which shows that the mean velocity in a near-wall region extending to around 700 “+” units in channels and ducts and 500 “+” units in pipes is the *same* as in the ZPG TBL. In other words, all the “canonical” flow profiles contain the lower end of the ZPG TBL log-region, which starts at a wall distance of 150–200 “+” units with a universal κ of $\kappa_{ZPG} \approx 0.384$. This interior log-region is followed by a second logarithmic region with a flow specific $\kappa > \kappa_{ZPG}$, which increases monotonically with pressure gradient. This second, exterior log-layer is the actual overlap layer matching up to the outer expansion, which implies equality of the exterior κ and κ_{CL} obtained from the evolution of the respective centerline velocity with Reynolds number. The location of the switch-over point implies furthermore that this second log-layer only becomes clearly identifiable, i.e., separated from the wake region, for Re_τ well beyond 10^4 (see Fig. 1). This explains the discrepancies between the Kármán constants of 0.38–0.39, extracted from near-wall pipe profiles below $Re_\tau \approx 10^4$ and the κ 's obtained from the evolution of the centerline velocity with Reynolds number. The same analysis is successfully applied to velocity profiles in channels and ducts even though experiments and numerical simulations have not yet reached Reynolds numbers where the different layers have even started to clearly separate.

DOI: [10.1103/PhysRevFluids.2.094602](https://doi.org/10.1103/PhysRevFluids.2.094602)

I. INTRODUCTION

After the formulation of the mixing length hypothesis and the logarithmic law $U^+ = \kappa^{-1} \ln(y^+) + B$ for a part of the mean velocity profile in wall-bounded turbulent flows by Prandtl [1] and von Kármán [2], the latter originally determined a value of 0.38 for κ , as pointed out by Segalini *et al.* [3]. Subsequently, however, $\kappa = 0.41$ became for a long time the most used value and almost acquired the aura of a fundamental physical constant. Here and in the following, “+” superscripts denote the usual wall scaling with friction velocity $\hat{u}_\tau \equiv (\hat{\tau}_{\text{wall}}/\hat{\rho})^{1/2}$ and kinematic viscosity $\hat{\nu}$, where “hats” denote dimensional quantities. The main reasons for this long period of constant κ has been the

*peter.monkewitz@epfl.ch

limited range of experimental Reynolds numbers and, probably more importantly, the use of the Clauser chart (Clauser [4], Wei *et al.* [5]) to determine the wall shear stress in turbulent boundary layers (TBLs).

With the advent of wall wires and, more commonly, the oil film technique, developed by Tanner and Blows [6], Fernholz *et al.* [7], and others, experimentalists have started to measure \hat{u}_τ in TBLs directly and most κ 's determined from high Reynolds number data have dropped into the 0.38–0.39 range. In pipes and channels, on the other hand, the spread of κ 's extracted from data has remained rather large, going from the original $\kappa = 0.436$ for the Princeton “Superpipe” (Zagarola and Smits [8]) to as low as 0.35–0.36 (Nagib and Chauhan [9]) for channels and high aspect ratio ducts. Despite a growing awareness of the effect of the log-law fitting range and other experimental parameters on κ (see, e.g., Örlü *et al.* [10], Segalini *et al.* [3]), the discrepancies have not gone away and today's turbulence community appears to be divided into essentially two camps: one advocating a universal κ , such as, for instance, Marusic *et al.* [11], and the other advocating flow-specific κ 's as expressed most clearly by Nagib and Chauhan [9].

In the context of singular perturbation theory, the logarithmic region is the link between inner and outer asymptotic expansions of the mean velocity $U_{\text{inner}}^+(y^+)$ and $U_{\text{outer}}^+(Y \equiv y^+/\text{Re})$, where Re is the Reynolds number $\text{Re}_{\delta_*} \equiv \hat{U}_\infty \hat{\delta}_*/\hat{\nu}$ based on free stream velocity and displacement thickness for the ZPG TBL and the friction Reynolds number or Kármán number Re_τ for channels and pipes. More precisely, the classical log-law is the common part U_{cp}^+ of U_{inner}^+ and U_{outer}^+ within the overlap layer $1 \ll y^+ \ll \text{Re}$. Since there are no independent “*a priori*” length scales, i.e., scales based on the operating parameters of the flow facility, between the inner scale $\hat{\nu}/\hat{u}_\tau$ and the boundary layer thickness, the two-term asymptotic expansion in powers of $\ln(\text{Re})$ of the free stream or centerline velocity necessarily has to be of the form $\kappa^{-1} \ln(\text{Re})$ plus a flow dependent constant, with the *same* κ as in the overlap layer. This is by no means new as it follows directly from Coles' [12] decomposition of the outer velocity into log-law and “wake” $U_{\text{outer}}^+ = \kappa^{-1} \ln(\text{Re} Y) + W(Y)$ evaluated at $Y = \text{const}$. Therefore, a universal κ for the log-laws in the zero pressure gradient turbulent boundary layer (ZPG TBL), the channel and the pipe necessarily implies that the free stream or centerline velocities in all three canonical flows *must* have the same logarithmic slope, which is contrary to the bulk of experimental evidence. The only possibility to reconcile a universal κ with the different Reynolds number dependence of the free stream or centerline velocities in the three flows considered here is to make the Coles wake function Re-dependent, of the form $W(Y, \text{Re})$, i.e., to add higher-order terms to the outer expansion. Such a possibility has been considered by Monkewitz and Nagib [13] and is further explored in Appendix B, without success.

Since experimental mean centerline and free stream velocities are the least affected by probe corrections, the present data reanalysis starts by fitting the available free stream or centerline data U_∞^+ or U_{CL}^+ with $\kappa^{-1} \ln(\text{Re}) + C$ and then proceeds to the near-wall log-laws. These freestream/centerline κ 's are distinctly different in the three canonical flows under study. So one must conclude that the log-law parameters, in particular the Kármán “coefficients” κ , are flow dependent. However, this conclusion is only final if one assumes, without necessity, that the velocity profile $U^+(y^+)$ contains only a single log region. As will be shown in this paper, the inner region of the overwhelming majority of high-quality mean velocity profiles in the Superpipe (Sec. III) and in channels/ducts (Sec. IV) is well described by inner expansions comprising *two* distinct parts: An interior near-wall part identical to the inner expansion of the ZPG TBL, reviewed in Sec. II, and an exterior log region with a flow specific Kármán “parameter” equal to the respective centerline κ_{CL} . For the pipe, this subdivision of the inner region is not entirely new, as both Zagarola and Smits [14] and McKeon *et al.* [15] have identified a change of the pipe velocity profiles from a power law to a log-law at $y^+ \approx 500$ without, however, connecting the interior part to the ZPG TBL profile. As the switch-over between the two regions is found at wall distances $y_{\text{int-ext}}^+$ of around 700 in channels and 500 in pipes, the interior region contains the beginning of the ZPG TBL log-law with its Kármán constant of $\kappa \cong 0.384$. Hence, in this restricted sense, the ZPG TBL log-law and its Kármán constant are universal. Beyond $y_{\text{int-ext}}^+$, however, the channel and pipe velocity profiles switch to flow specific logarithmic laws with flow specific Kármán “parameters” equal to the respective centerline κ_{CL} 's,

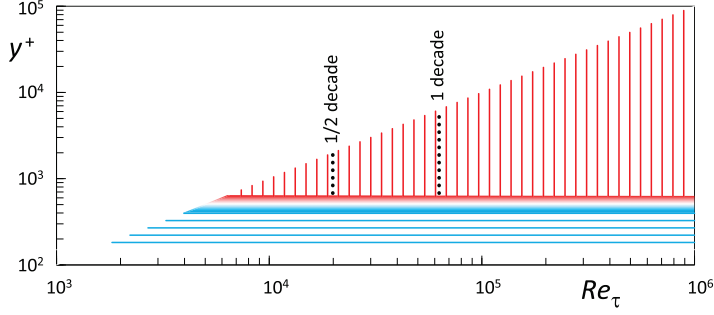


FIG. 1. The two logarithmic regions, as identified in Sec. III for the pipe: universal interior log region (horizontal hatching) with $\kappa = 0.384$ for $200 \lesssim y^+ \lesssim y_{\text{int-ext}}^+ \approx 500$, exterior (vertical hatching) overlap layer with $\kappa = \kappa_{\text{CL}}$ for $y_{\text{int-ext}}^+ \leq y^+ \lesssim 0.1 \text{Re}_\tau$ and transition layer (shaded). . . , minimum Re_τ 's to see one half and one decade of “clean” overlap log-law.

as shown in Fig. 1. The figure also shows that the exterior log layers, which are the actual overlap layers matching up to the respective outer expansions, require relatively high Re_τ , in excess of 10^4 , to clearly separate from the wake. Only in the ZPG TBL, the interior and exterior log regions are one and the same.

II. THE MEAN VELOCITY PROFILE IN THE ZPG TBL

The point to be reiterated here is the equality in the ZPG TBL of the κ 's in the log-law and in the expression for the free-stream velocity $U_\infty^+(\text{Re}_{\delta_*})$.

This is achieved by showing that the mean velocity data set used by Bailey *et al.* [16], which is probably the most thoroughly checked data set, together with the data of Kulandaivelu [17] are nearly perfectly matched by a composite expansion consisting of the modified “Musker” fit for $U_{\text{inner,ZPG}}^+$, developed by Chauhan *et al.* [18] and reproduced for convenience in Appendix A, and a new fit for the outer velocity $U_{\text{outer,ZPG}}^+(\eta)$, with $\eta \equiv y^+/\text{Re}_{\delta_*}$ the outer wall-normal coordinate according to Rotta [19]:

$$U_{\text{outer,ZPG}}^+(\eta) = \frac{\ln\{3.50 \text{Re}_{\delta_*} \times \tanh^{1/2}[f(\eta)]\}}{0.384}, \quad \text{with}$$

$$f(\eta) = \left(\frac{5.05 \eta}{3.50}\right)^2 \frac{1 + (10.7 \eta)^4 + (11.9 \eta)^5 + (10.7 \eta)^8}{1 + (11.9 \eta)^5} \quad (1)$$

$$U_{\text{outer,ZPG}}^+(\eta \ll 1) \sim U_{\text{log,ZPG}}^+ + (11.4 \eta)^4 + \dots, \quad \text{with}$$

$$U_{\text{log,ZPG}}^+ \equiv U_{\text{cp,ZPG}}^+ = \frac{1}{0.384} \ln(y^+) + 4.22, \quad (2)$$

$$U_{\text{outer,ZPG}}^+(\eta \rightarrow \infty) \equiv U_\infty^+ = \frac{1}{0.384} \ln(\text{Re}_{\delta_*}) + 3.26. \quad (3)$$

Eq. (1) is simpler than most previous fits, avoids the introduction of a rather arbitrary boundary layer thickness δ , has equal κ 's in the common part $U_{\text{log,ZPG}}^+$ [Eq. (2)] of inner and outer expansions and U_∞^+ [Eq. (3)] and satisfies the asymptotic consistency requirement $\int_0^\infty (U_\infty^+ - U_{\text{outer,ZPG}}^+) d\eta = 1$ within 0.15% (see Monkewitz *et al.* [20]). The near perfect data fit can be appreciated in Fig. 2. Note also that the fit by Eq. (1) is likely the first to correctly reproduce the departure from the log-law $\propto \eta^4$ at large y^+ , shown in Fig. 2(a) and achieved by the “trick” of using the square root $\tanh^{1/2}(\eta^2 \dots)$ in Eq. (1).

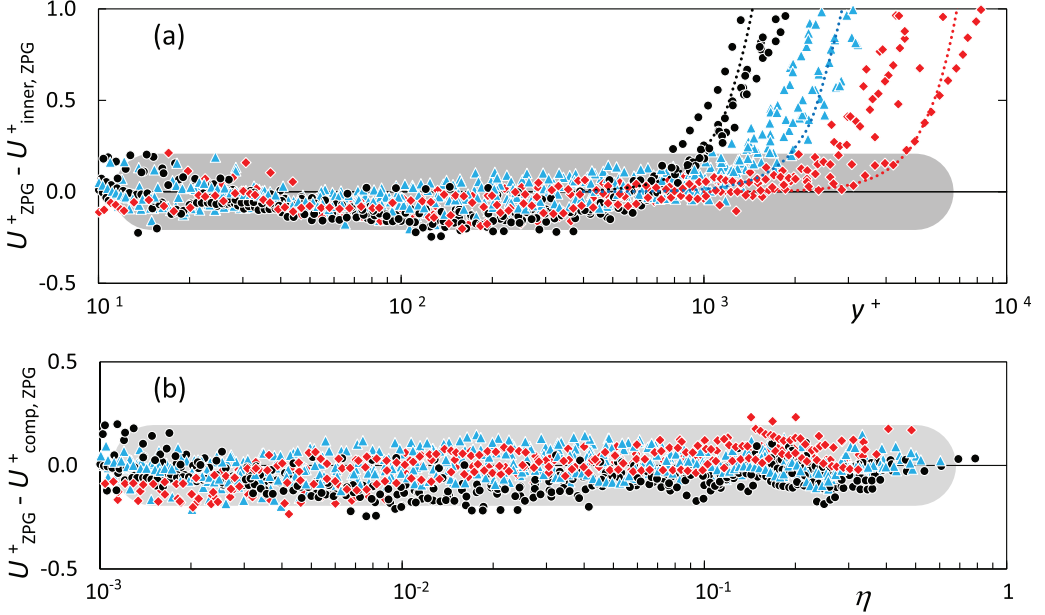


FIG. 2. (a) Nineteen ZPG TBL mean velocity profiles used by Bailey *et al.* [16] to elucidate Pitot corrections and six profiles of Kulandaivelu [17] minus the Musker inner fit $U^+_{inner,ZPG}$ [Eq. (A1)]. \bullet , $Re_{\delta_*} \leq 2 \times 10^4$; \blacktriangle , $2 \times 10^4 < Re_{\delta_*} \leq 4 \times 10^4$; \blacklozenge , $Re_{\delta_*} > 4 \times 10^4$. \cdots , leading term $(11.4 \eta)^4$ of the small- η expansion [Eq. (2)] of $(U^+ - U^+_{inner,ZPG})$ for $Re_{\delta_*} = 1.65 \times 10^4$ (last black profile), 3.26×10^4 (last blue profile), and 7.84×10^4 (last red profile). (b) Corresponding experimental profiles minus the composite expansion $(U^+_{inner,ZPG} + U^+_{outer,ZPG} - U^+_{cp,ZPG})$ [Eqs. (A1), (1) and (2)] versus η . The gray bands indicate deviations of up to ± 0.2 from the inner expansion in (a) and from zero in (b).

Before moving on to the analysis of pipe and channel data, a few comments are called for. Here and in the following, the value of $\kappa = 0.384$ determined by Monkewitz *et al.* [20] is used for the ZPG TBL and the interior log-laws to be identified in pipes and channels. It is clear that the third digit of κ depends on the choice of data, but its value is now generally thought to be in the interval $[0.38, 0.39]$ (see, e.g., Marusic *et al.* [21]). As the standard oil film technique to measure wall shear stress leads to a slight systematic over-estimate of κ (Segalini *et al.* [22]), the value of 0.384 is preferred over 0.39.

Finally, since past comparisons with pipe and channel have often been made on the basis of equal Re_τ , variously defined in the TBL as $\eta_{.99} \times Re_{\delta_*}$ or $\eta_{.995} \times Re_{\delta_*}$, it is useful to recall that these quantities, besides being strongly affected by measurement uncertainties and/or data fits, do not correspond to fixed values of the outer variable η . In other words, scaling arguments based on Re_{δ_*} and Re_τ are not equivalent if they are supposed to be valid to infinite Reynolds number. For the present fit by Eq. (1), $\eta_{.99}$ and $\eta_{.995}$ decrease appreciably from 0.232 and 0.245 at $Re_{\delta_*} = 10^4$ to, respectively, 0.213 and 0.231 at $Re_{\delta_*} = 10^9$, as shown in Fig. 3.

III. THE MEAN VELOCITY PROFILE IN PIPES, WITH EMPHASIS ON THE PRINCETON SUPERPIPE

There exists a large number of turbulent pipe flow experiments, the best known early study being the one by Nikuradse [23]. As the aim of this section is to investigate the relation between the κ 's extracted from the logarithmic region of $U^+(y^+)$ and from the centerline velocity $U^+_{CL,P}(R^+)$, with $R^+ \equiv (\widehat{R} \widehat{u}_\tau / \widehat{\nu}) \equiv Re_\tau$ the nondimensional pipe radius and relevant Reynolds number, the requirements on the data are severe. On the one hand, the Reynolds numbers must be sufficiently

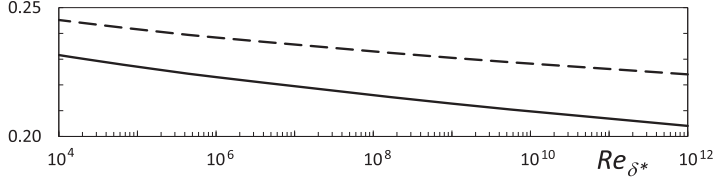


FIG. 3. Boundary layer thicknesses $\eta_{.99}$ (—) and $\eta_{.995}$ (- -) versus Re_{δ^*} for the outer fit [Eq. (1)].

high, at least of the order of 10^4 , to obtain a substantial logarithmic region in the profile $U^+(y^+)$. On the other hand, the data must cover a large range of R^+ : As $U_{CL,P}^+$ is asymptotically $\propto \ln(R^+)$, one decade of R^+ corresponds to an increase of $U_{CL,P}^+$ by only about 5, so that an uncertainty of ± 0.2 in $U_{CL,P}^+$ translates to a 7% uncertainty in κ . For these reasons, the following data analysis will focus on the Superpipe data (see Zagarola and Smits [8,14] for a description of the facility).

Other investigations of high Reynolds number pipe flow are under way, but have not yet produced data sets comparable to the Superpipe. Among them is an effort by a Japanese group (Furuichi *et al.* [24]) which has so far published mean velocity data up to $R^+ \approx 10^4$ (corresponding to the lowest blue Superpipe profile in Fig. 5). Furthermore, the publication concentrates on friction factor correlations based on bulk velocity and does not directly provide data for the centerline velocity. The CICLoPE experiment (see Talamelli *et al.* [25]), with a somewhat smaller Reynolds number range than the Superpipe, is currently starting up in Italy and the first preliminary centerline data of Fiorini [26] in the range $10^4 \leq R^+ \leq 4 \times 10^4$ yield a κ of 0.437 (see Fig. 4), which is significantly larger than the κ of 0.39 deduced from the near-wall log-layer by Örlü *et al.* [27] in the same facility. This discrepancy between the κ 's determined from the logarithmic region of U^+ and from the centerline velocity has already been noticed by Zanoun *et al.* [28], despite a limited Reynolds number range of $R^+ < 9000$.

The Superpipe data have had a major impact on turbulence research due to the dramatic increase of R^+ over previous studies, but two features of these experiments have given rise to much scrutiny and debate:

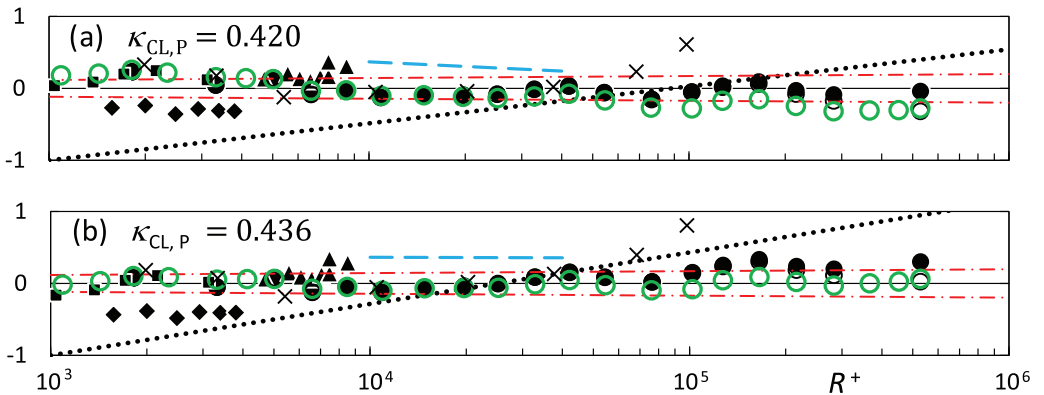


FIG. 4. Experimental pipe centerline velocities versus R^+ with a Hama-like roughness correction $(2\kappa)^{-1} \ln[1 + (0.14 k_s^+)^2]$ ($\hat{k}_s = 0.45 \mu\text{m}$) minus the fit [Eq. (4)] for $U_{CL,P}^+$ in panel (a); minus the fit $(1/0.436) \ln(R^+) + 7.65$ of Zagarola and Smits [8] in (b). •, Superpipe data corrected according to McKeon; ○, same data without roughness correction; ◊, Superpipe data of Zagarola and Smits [8] with same roughness correction; ×, Superpipe NSTAP data of Hultmark *et al.* [34]; ◆, Perry and Abell [35]; ▲, Zanoun *et al.* [28]; ■, Monty [36]; - - -, preliminary CICLoPE correlation $(1/0.437) \ln(R^+) + 8.06$ of Fiorini [26]; - · - ·, $\pm 0.5\%$ of reference $U_{CL,P}^+$. · · · ·, slope corresponding to $\kappa = 0.384$.

(1) One problem was the very large diameter of the Pitot probes in viscous units, which decrease to $0.6 \mu\text{m}$ at the higher R^+ 's, and required the extension of the correction schemes for mean shear, viscous effects and turbulence intensity into uncharted territory. This issue has been addressed by McKeon and Smits [29] and McKeon *et al.* [30], using the argument that $U^+(y^+)$ in the wall region is universal and must be independent of the Pitot probe diameter, and more recently by an international collaboration (Bailey *et al.* [16]), which relied on the comparison between Pitot and hot-wire measurements in ZPG TBL's. In addition, Vinuesa *et al.* [31] have investigated the effect of possible Pitot positioning errors. These different efforts have led to a fair agreement on the most appropriate corrections, albeit the uncertainty of the Superpipe data remains relatively large for $y^+ \lesssim 10^3$ in comparison with data sets at lower Reynolds numbers, such as those included in Fig. 4. Beyond $y^+ \approx 10^3$, however, the corrections quickly become small.

(2) The second issue was the influence of roughness at the higher R^+ which has been thoroughly studied by Allen *et al.* [32]. As a result, there is now widespread agreement that only the profiles with $R^+ \gtrsim 2 \times 10^5$ are significantly affected by roughness.

A. The log-law for the pipe centerline velocity

Starting with the centerline velocity $U_{\text{CL,P}}^+$ and excluding the lowest as well as the three highest R^+ , where the roughness correction increases the uncertainty, the Pitot data are least-squares fitted by

$$U_{\text{CL,P}}^+ = \frac{1}{0.42} \ln(R^+) + 6.84, \quad (4)$$

with an R^2 value of 0.9993. As can be appreciated in Fig. 4(a), all the Superpipe Pitot data beyond the lowest Reynolds number are within $\pm 0.5\%$ of the fit Eq. (4), if corrected for roughness with a Hama-like roughness correction $(2\kappa)^{-1} \ln[1 + (0.14k_s^+)^2]$ and $\hat{k}_s = 0.45 \mu\text{m}$, in line with the investigation of Allen *et al.* [32]. If all 19 data points are used, the least-squares κ increases insignificantly to 0.423. As evidence from CICLoPE (see Fiorini [26]) is mounting that the centerline $\kappa_{\text{CL,P}}$ may be as high as 0.44, in almost perfect agreement with the original data of Zagarola and Smits [14], the same data as in (a) minus the fit $U_{\text{CL,P}}^+ = (1/0.436) \ln(R^+) + 7.65$ of Zagarola and Smits [14] are shown in Fig. 4(b). What is obvious from Fig. 4 is that determining the centerline κ within, say, ± 0.01 from any individual data set requires a Reynolds number span of a decade or more and an extreme attention to all, even small, systematic errors. Nevertheless, Fig. 4 demonstrates convincingly, that $\kappa_{\text{CL,P}} = 0.42$ is the lowest value compatible with data, i.e., that $\kappa_{\text{CL,P}}$ in the pipe is significantly larger than the κ in the ZPG TBL.

Comparing with other experiments, it is remarkable that the fit by Eq. (4) is essentially identical to the fit of $U_{\text{CL,P}}^+$ in Fig. 38 of Nikuradse [23] over the range $10^2 \leq R^+ \leq 5 \times 10^4$ and given as $(1/0.417) \ln(R^+) + 6.84$ (note the typo 5.84 instead of 6.84 for the additive constant on p. 66 of the NASA translation). The κ in Eq. (4) is also virtually identical to the $\kappa = 0.421$ fitted by McKeon *et al.* [15] to the logarithmic region beyond $y^+ \gtrsim 600$ and is consistent with the values estimated by Bailey *et al.* [33, see in particular their Fig. 4(b)], except for the values extracted from the new NSTAP ‘‘micro-hotwire’’ data of Hultmark *et al.* [34]. The latter data are also included in Fig. 4 to support the opinion of this author that the NSTAP technology is not yet sufficiently validated to reliably deduce Kármán constants: Using all eight NSTAP data points yields a least-squares κ of 0.41, while the four lowest and highest R^+ yield κ 's of 0.47 and 0.36, respectively. Finally, it is noted that the various data sets in Fig. 4 below R^+ of 10^4 are compatible with $\kappa \geq 0.42$, but too short to extract a reliable value.

B. The ‘‘interior’’ and ‘‘exterior’’ log regions

Turning the attention to the near-wall region of $U^+(y^+)$, the Superpipe data are less helpful below $y^+ \approx 10^3$ for the reasons discussed at the beginning of Sec. III. At low y^+ , below around 600, both Zagarola and Smits [14] and McKeon *et al.* [15] see a power law, but the latter authors remark that

in the interval $350 < y^+ < 950$ a log-law with $\kappa = 0.385$ and an additive constant of 4.15 “fits the data quite well.”

From the point of view of balance of terms in the Reynolds averaged momentum equation, the mean velocities in pipe and channel flows should, in wall units, be virtually identical to the ZPG TBL mean velocity in the region where the viscous and Reynolds stresses dominate over the pressure gradient, which is of order $\mathcal{O}(1/R^+)$. In pipe flow, this is the region outside a very thin wall sublayer in which the viscous stress is balanced by the pressure gradient (see Klewicki *et al.* [37] and references therein). The thickness y_{pgsl}^+ , with “pgsl” for pressure gradient sublayer, is obtained as the wall distance at which the pressure gradient term is equal to the second derivative of the $(y^+)^4$ term in the Taylor series of the ZPG TBL mean velocity about the wall. Using table 2 of Monkewitz and Nagib [38], one obtains $y_{\text{pgsl}}^+ \approx 10^2/\sqrt{R^+}$, which is so small that this layer has no measurable effect on experimental velocity profiles much beyond y_{pgsl}^+ . So the dominant balance in the inner region of pipe flow, outside of this pressure gradient sublayer, is the same as in the ZPG TBL, where the convective terms and the stream-wise stress derivatives in the inner, near-wall region are small of order $\mathcal{O}[\text{Re}_{\delta_*} \ln^2(\text{Re}_{\delta_*})]^{-1}$ (see Monkewitz and Nagib [38]).

Therefore, as long as the pressure gradient in the momentum equation remains sufficiently smaller than the viscous and Reynolds stresses, one expects to see in the pipe (and in the channel) the same mean velocity profile as in the ZPG TBL with a logarithmic region of slope $1/0.384$ beyond $y^+ \approx 150\text{--}200$. Indeed, such a logarithmic region with κ 's in the range $0.38\text{--}0.39$ has been clearly identified in many pipe flow studies at lower $R^+ \lesssim 10^4$, where the logarithmic overlap layer does not extend beyond $y^+ \approx 10^3$ and probe correction problems are minor compared to the Superpipe: Monty [36], for instance, identified a log-law for $y^+ \gtrsim 150$ with $\kappa = 0.384$ and 0.386 , using hot-wires and Pitot tubes, respectively, Zanoun *et al.* [28] found κ 's between 0.38 and 0.39 depending on the fitting range, Furuichi *et al.* [24] deduced a κ of 0.382 from their profiles and Örlü *et al.* [27] found 0.39 from CICLoPE near-wall profiles for $R^+ \leq 3.2 \times 10^4$.

As there is no reason for the near-wall profiles $U^+(y^+)$ in the Superpipe to be different from the profiles in experiments with R^+ between 10^3 and 10^4 , such as the ones mentioned above, the Superpipe profiles must also have an interior log region with a κ of around 0.384 which is just somewhat difficult to identify due to the residual uncertainty of the Pitot corrections. To reveal this interior log region, the inner expansion $U_{\text{inner,ZPG}}^+$ [Eq. (A1)] of the ZPG TBL is first subtracted from the Superpipe Pitot data, corrected according to McKeon *et al.* [30] and the result is shown in Fig. 5. The implementations of the Pitot corrections by Bailey *et al.* [16] and Vinuesa and Nagib [39], included in Fig. 5 for $y^+ \leq 10^3$, are seen to mainly shift the graphs down by $0.1\text{--}0.15$.

The most striking feature of Fig. 5 is the rather abrupt and simultaneous switchover at $y^+ = \mathcal{O}(10^3)$ of all the profiles with $R^+ \gtrsim 10^4$ to an exterior log-law, the actual logarithmic overlap layer, with the same logarithmic slope of $(1/0.420)$ as in Eq. (4) for $U_{\text{CL,P}}^+$. Note again that the data for $R^+ < 10^4$ cannot show this second log region, because $y^+ = 10^3$ corresponds already to $Y \geq 0.1$, which is at or beyond the upper end of any log-law.

The smooth switch from interior to exterior log region in Fig. 5 is well modeled by

$$\begin{aligned} \Delta U_{\text{log,P}}^+ &= \left(\frac{1}{0.384} - \frac{1}{0.420} \right) \frac{\ln[1 + (0.002 y^+)^3]}{3} \\ &\sim 0.223 \ln[0.002 y^+] \quad \text{for } (0.002 y^+) \gg 1, \end{aligned} \quad (5)$$

which places the boundary between the two log regions at $y_{\text{int-ext}}^+ = 1/0.002 = 500$.

To reinforce the point about the Pitot corrections becoming noncontroversial beyond $y^+ \approx 10^3$, the Pitot data, corrected according to both McKeon and Bailey, minus $U_{\text{inner,ZPG}}^+$ [Eq. (A1)] are shown in Fig. 6 for the interval $3(R^+)^{1/2} \leq y^+ \leq 0.15R^+$. This is the extent of the unique and universal logarithmic region with $\kappa = 0.39$, claimed by Marusic *et al.* [11] to exist in all three canonical flows. To understand this claim, the Superpipe data in their Fig. 1, together with the original NSTAP data of Hultmark *et al.* [34], are included in Fig. 6(a). These latter data are seen to be the only ones

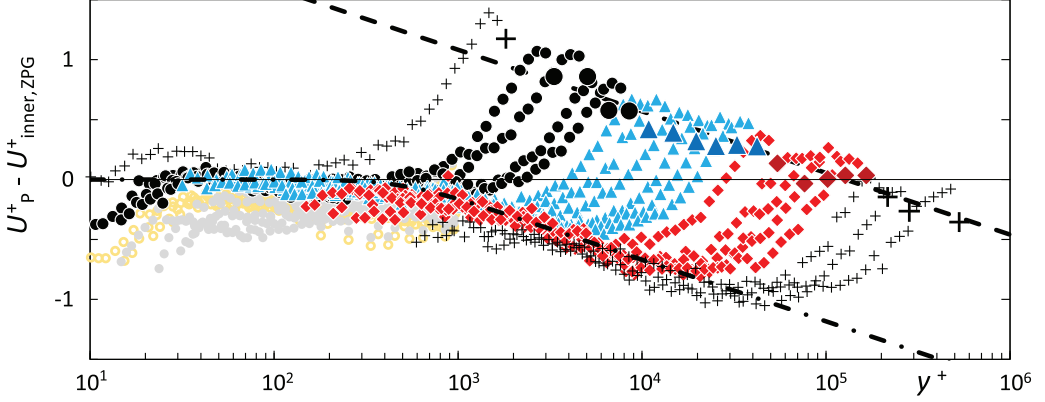


FIG. 5. Nineteen Superpipe profiles minus the ZPG TBL inner expansion [Eq. (A1)], $U^+ - U_{\text{inner,ZPG}}^+$, versus y^+ , with Pitot corrections according to McKeon and the Hama-like roughness correction given in the caption of Fig. 4. +, $R^+ = 1.82 \times 10^3$ considered low Reynolds number; ●, $R^+ = \{3.31, 5.08, 6.58, 8.49\} \times 10^3$; ▲, $R^+ = \{1.09, 1.48, 1.97, 2.51, 3.27, 4.21\} \times 10^4$; ◆, $R^+ = \{0.542, 0.761, 1.02, 1.27, 1.65\} \times 10^5$; +, $R^+ = \{2.16, 2.83, 5.27\} \times 10^5$ where roughness effects become significant. Corresponding large symbols mark the centerline. Gray ●, ○, same data for $3 \times 10^3 < R^+ < 2 \times 10^5$ corrected according to Vinuesa-Nagib and Bailey, respectively. - - -, $U_{\text{CL,P}}^+ - U_{\text{inner,ZPG}}^+$ for $R^+ \gg 1$; - · -, $(-\Delta U_{\log,\text{P}}^+)$ given by Eq. (5) for $R^+ \gg 1$.

supporting a single universal log-law with $\kappa = 0.39$ beyond y^+ of 10^3 . As they were obtained with a radically new probe for which experience is still limited and which does not yield a clear log-law for $U_{\text{CL,P}}^+$, as discussed in Sec. III A, they will not be considered further in the present study.

Returning to the Pitot data with the two log regions of Fig. 5, the basic question arises whether the first or the second logarithmic region corresponds to the common part of the inner and outer expansions of U^+ :

(1) The fact that the switch over occurs, within experimental error, at a fixed y^+ is a strong indication that the overlap region corresponds to the second log region with $\kappa = 0.420$, consistent with the logarithmic slope of $U_{\text{CL,P}}^+$ in Eq. (4).

(2) The alternative, i.e., a universal common part with $\kappa = 0.384$, implies that the asymptotic expansion of $U_{\text{CL,P}}^+$ would have to be of the form $(1/0.384) \ln(R^+) + \text{const.} + \text{HOT}$, where HOT

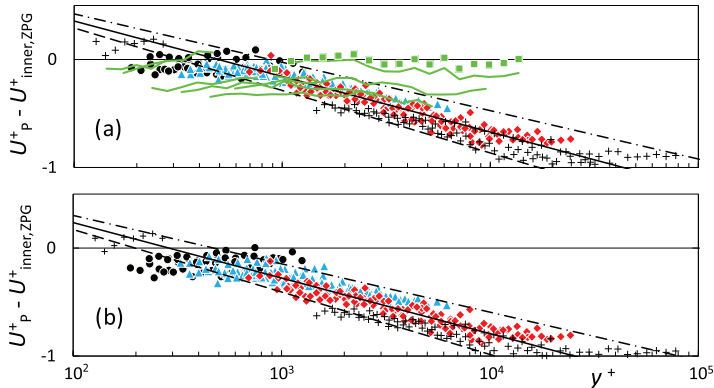


FIG. 6. $(U^+ - U_{\text{inner,ZPG}}^+)$ [Eq. (A1)] versus y^+ for $3(R^+)^{1/2} \leq y^+ \leq 0.15R^+$. (a) Symbols of Fig. 5: Pitot data corrected according to McKeon *et al.* [30]; —, original NSTAP data from Hultmark *et al.* [34]; ■, NSTAP data for $R^+ = 9.82 \times 10^4$ from Marusic *et al.* [11]. Slopes corresponding to $\kappa = 0.425$ (—), 0.42 (—) and 0.415 (- · -). (b) Analogous to (a) but with Pitot data corrected according to Bailey *et al.* [16].

stands for higher-order term, because the two-term expansion without the HOT is not defensible on the basis of Fig. 4 and the discussion in Sec. III A. As shown by Monkewitz and Nagib [13] (see Fig. 10 in Appendix B), a third term of order $\mathcal{O}(\ln R^+)^{-1}$ in Eq. (B1) does a good job at fitting the available centerline data, but the corresponding outer expansion Eq. (B2) fails to describe the observed outer profiles.

The conclusion from the above discussion is that the interior log region with $\kappa = 0.384$ in pipe flow is a feature of the inner expansion of U_p^+ and that the log region with $\kappa = 0.420$ is the actual overlap region, i.e., the common part of inner and outer pipe expansions. In other words, the inner expansion for the mean velocity in the pipe is given by

$$U_{\text{inner,P}}^+ \equiv U_{\text{inner,ZPG}}^+ - \Delta U_{\text{log,P}}^+, \quad (6)$$

with $\Delta U_{\text{log,P}}^+$ given by Eq. (5). Finally, the common part of inner and outer expansions for U_p^+ is obtained by taking the limit $y^+ \gg 500$ of Eq. (6),

$$U_{\text{cp,P}}^+ \equiv \lim_{y^+ \rightarrow \infty} U_{\text{inner,P}}^+ \sim \frac{1}{0.42} \ln(y^+) + 5.604, \quad (7)$$

which has to correspond to the limit $Y \ll 1$ of $U_{\text{outer,P}}^+$ developed in the next section.

C. The outer expansion

The remaining task is to find a suitable outer expansion for U_p^+ . For this, the complete inner pipe expansion $U_{\text{inner,P}}^+$ [Eq. (6)] is subtracted from U_p^+ , as shown in Fig. 7(a), which is obtained from Fig. 5 by “lifting” the data by $\Delta U_{\text{log,P}}^+$. This yields $U_{\text{outer,P}}^+ - U_{\text{cp,P}}^+$, which is easily fitted by

$$U_{\text{outer,P}}^+(Y) - U_{\text{cp,P}}^+ = \frac{1}{0.420} \ln \left[\left(\frac{\pi}{2} Y \right)^{-1} \sin \left(\frac{\pi}{2} Y \right) \right] + 2.30 \sin^2 \left(\frac{\pi}{2} Y \right). \quad (8)$$

As seen in Fig. 7(b), the composite expansion $U_{\text{comp,P}}^+(Y) \equiv U_{\text{inner,P}}^+ + U_{\text{outer,P}}^+ - U_{\text{cp,P}}^+$ fits all the Superpipe profiles with an absolute error below ± 0.2 . Furthermore, it follows from the Taylor series expansion of $U_{\text{outer,P}}^+$ that the initial deviation of $U_{\text{outer,P}}^+$ from $U_{\text{cp,P}}^+$ in the pipe is much more gradual than in the ZPG TBL, i.e., $\propto Y^2$ as opposed to $\propto \eta^4$ in the ZPG TBL.

IV. THE MEAN VELOCITY PROFILE IN CHANNELS AND DUCTS

Below $\text{Re}_\tau \equiv H^+ \approx 1000$ (H^+ being the nondimensional channel/duct half height) the U^+ -profiles in ducts become progressively affected by the duct aspect ratio, as documented by Vinuesa *et al.* [40] and [41]. Hence, attention is focused here on the Reynolds number range $H^+ \geq 950$, where the difference between U^+ from channel DNS and duct experiments is of the order of the experimental uncertainty. For the following analysis, six profiles from channel DNS's of Hoyas and Jiménez [42], Lozano-Durán and Jiménez [43], Lee and Moser [44], and Thais *et al.* [45], with $950 \leq H^+ \leq 5200$, are used, together with four experimental profiles of Zanoun *et al.* [46] for $2155 \leq H^+ \leq 4783$ and another four of Schultz and Flack [47] for $1010 \leq H^+ \leq 5900$.

For channels and ducts there are no data at high enough H^+ to reveal a double log region as in Fig. 5 for the Superpipe. As a matter of fact, the available H^+ are still too low to even see a clear log-law in the $U^+(y^+)$ profiles and so there has not yet been any controversy about a difference between κ 's extracted from the near-wall logarithmic region and from $U_{\text{CL,Ch}}^+$, even though Schultz and Flack [47] found a κ from the friction factor which was higher by 0.02 than the one obtained from their profiles. The fortunate difference to the pipe is the availability of high quality DNS channel data over the entire H^+ -range of the laboratory experiments, which allow a reliable fit of $U_{\text{CL,Ch}}^+$, despite the limited range of H^+ . The best fit for the DNS channel data above $H^+ = 950$, with an R^2 value of 0.9998 is

$$U_{\text{CL,Ch}}^+ = \frac{1}{0.413} \ln(H^+) + 5.88. \quad (9)$$

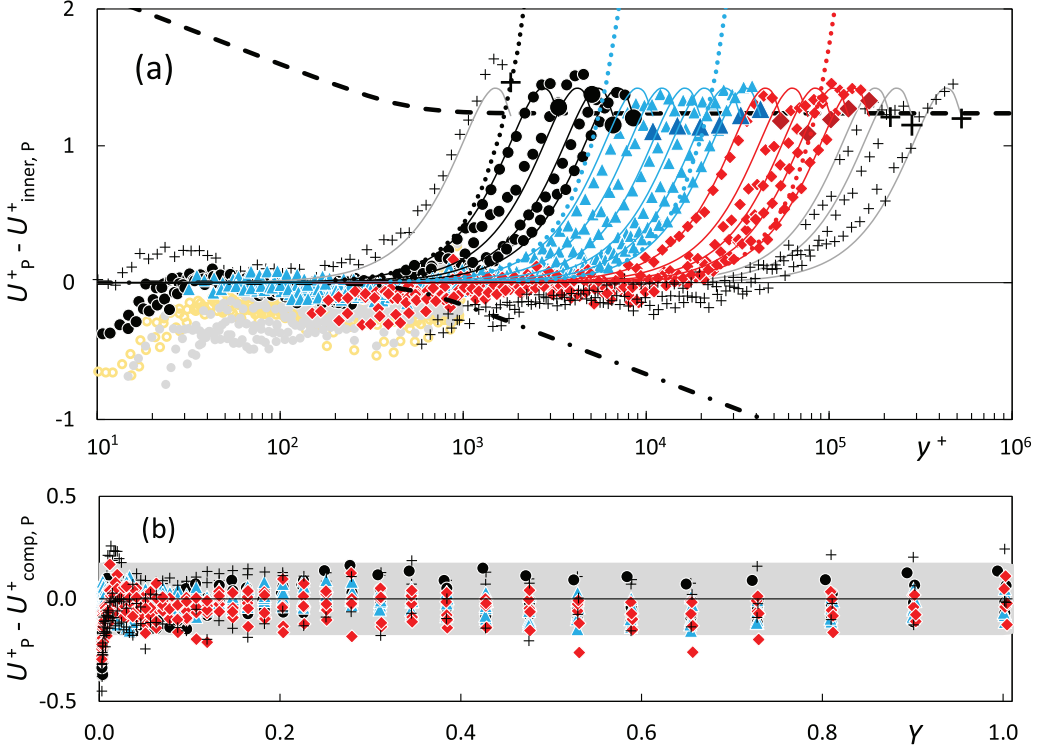


FIG. 7. (a) Superpipe profiles of Fig. 5 plus $\Delta U_{\log,P}^+$ (Eq. 5). Thin gray lines, $(U_{\text{outer},P}^+ - U_{\text{cp},P}^+)$ [Eq. (8)], \dots , leading term ($4.70 Y^2$) of the Taylor expansion of $(U_{\text{outer},P}^+ - U_{\text{cp},P}^+)$ for $R^+ = 3.31 \times 10^3$ (first black profile), 1.09×10^4 (first blue profile), 4.21×10^4 (last blue profile), and 1.65×10^5 (last red profile). (b) Data minus the composite expansion $U_{\text{comp},P}^+ \equiv U_{\text{inner},P}^+ + U_{\text{outer},P}^+ - U_{\text{cp},P}^+$ [Eqs. (6), (8) and (7)]. The gray band indicates deviations of up to ± 0.2 from zero. See caption of Fig. 5 for other symbols.

As seen in Fig. 8, the experimental $U_{\text{CL,Ch}}^+$ have a much larger scatter and fall generally below the DNS fit, which is interpreted as a remnant of the aspect ratio effect.

Focussing on the DNS by Lee and Moser [44] at $H^+ = 5200$, a nascent interior log-law with the ZPG TBL parameters is evident in Fig. 9(a), but there is no sign yet of an exterior logarithmic overlap layer with $\kappa = 0.413$ to match $U_{\text{CL,Ch}}^+$. From the asymptotic matching argument in Sec. I, one must therefore conclude that, at the available H^+ 's, the exterior log region is “telescoped” into the wake and that the two regions will only separate at considerably higher H^+ 's (see Fig. 1). This does, however, not preclude the use of the same asymptotic description of the mean velocity profile as for the pipe, since asymptotic expansions generally provide useful approximations already before

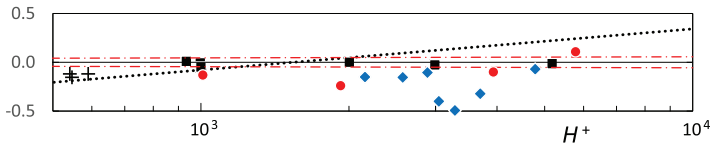


FIG. 8. Channel/duct centerline velocity of the profiles in Fig. 9 minus the fit by Eq. (9) for $U_{\text{CL,Ch}}^+$ versus H^+ . \blacksquare , DNS channel data for $H^+ \geq 950$; \bullet , Schultz and Flack [47]; \blacklozenge , Zanoun *et al.* [46]. See caption of Fig. 9 for more details. $+$, DNS data at $H^+ = 550$ and 590 not considered for the fit. $-\cdot-\cdot-$, $\pm 0.2\%$ of $U_{\text{CL,Ch}}^+$ [Eq. (9)]. \dots , slope corresponding to $\kappa = 0.384$.

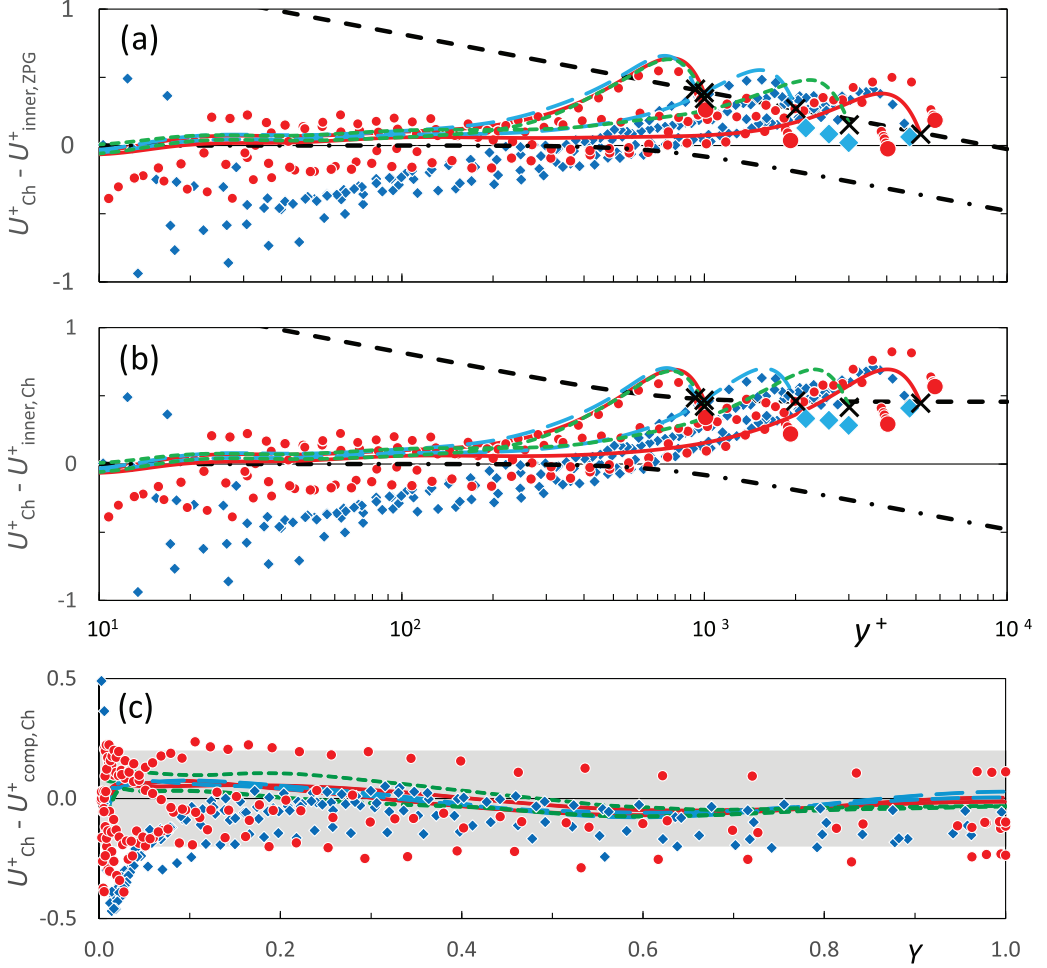


FIG. 9. Six DNS profiles of Hoyas and Jiménez [42] (— —), Thais *et al.* [45] (- - -) and Lee and Moser [44] (—), four profiles of Schultz and Flack [47] (●) and four profiles of Zanoun *et al.* [46] (◆). (a) $(U^+ - U^+_{inner,ZPG})$ [Eq. (A1)] versus y^+ ; - · - ·, $-\Delta U^+_{log,Ch}$ (Eq. 10); - - -, centerline velocity [Eq. (9)] minus $U^+_{cp,ZPG}$ [Eq. (2)]. (b) $U^+ - U^+_{inner,Ch}$ [Eq. (11)]. (c) $U^+ - U^+_{comp,Ch}$ [Eqs. (11) plus (12)]. The grey band indicates deviations of up to ± 0.2 from zero.

the different regions (here the exterior log region and the wake) are clearly separated [see, e.g., the surprisingly good outer fit of the low- R^+ data in Fig. 7(a)].

Hence, proceeding as for the pipe, the inner expansion for $U^+_{inner,ZPG}$ [Eq. (A1)] is again subtracted first from the data and the remainder is “lifted” by the channel equivalent of Eq. (5),

$$\begin{aligned} \Delta U^+_{log,Ch} &= \left(\frac{1}{0.384} - \frac{1}{0.413} \right) \frac{\ln[1 + (0.0014 y^+)^3]}{3} \\ &\sim 0.183 \ln[0.0014 y^+] \quad \text{for } (0.0014 y^+) \gg 1, \end{aligned} \quad (10)$$

to yield the inner expansion for the channel

$$U^+_{inner,Ch} = U^+_{inner,ZPG} - \Delta U^+_{log,Ch}. \quad (11)$$

TABLE I. Summary for the three canonical flows of the parameters for the interior log-law $\kappa_{\text{int}}^{-1} \ln(y^+) + B_{\text{int}}$, the switch-over point $y_{\text{int-ext}}^+$ from interior to exterior log-law, the parameters for the exterior log-law $\kappa_{\text{ext}}^{-1} \ln(y^+) + B_{\text{ext}}$ and the additive constant for U_{∞}^+ , respectively, $U_{\text{CL}}^+ = \kappa_{\text{ext}}^{-1} \ln(\text{Re}_{\tau}) + C$.

	β	κ_{int}	B_{int}	$y_{\text{int-ext}}^+$	κ_{ext}	B_{ext}	C
ZPG TBL	0	0.384	4.22	—	0.384	4.22	3.26
Channel	1	0.384	4.22	≈ 700	0.413	5.42	5.88
Pipe	2	0.384	4.22	≈ 500	0.420	5.60	6.84

Note that in Eq. (10) the switch-over point between the interior and exterior log layers has been placed at $y^+ = (0.0014)^{-1} \approx 700$, as opposed to ≈ 500 in the pipe (see discussion in Sec. V). Analogous to Eq. (8), the difference $U_{\text{outer,Ch}}^+ - U_{\text{cp,Ch}}^+$ is fitted by

$$U_{\text{outer,Ch}}^+(Y) - U_{\text{cp,Ch}}^+ = \frac{1}{0.413} \ln \left[\left(\frac{\pi}{2} Y \right)^{-1} \sin \left(\frac{\pi}{2} Y \right) \right] + 1.55 \sin^2 \left(\frac{\pi}{2} Y \right), \quad (12)$$

with

$$U_{\text{cp,Ch}}^+ = \frac{1}{0.413} \ln(y^+) + 5.419. \quad (13)$$

As in Figs. 5 and 7 for the pipe, Fig. 9(a) shows selected channel and duct mean velocity profiles minus $U_{\text{inner,ZPG}}^+$ [Eq. (A1)] and Fig. 9(b) the profiles minus the complete inner expansion [Eq. (11)]. Figure 9(c) for $(U_{\text{Ch}}^+ - U_{\text{comp,Ch}}^+)$, finally, demonstrates the excellent quality of the composite fit $U_{\text{comp,Ch}}^+ \equiv U_{\text{inner,Ch}}^+ + U_{\text{outer,Ch}}^+ - U_{\text{cp,Ch}}^+$ for the DNS channel profiles in particular. As in Fig. 8, all but one experimental difference $(U^+ - U_{\text{comp,Ch}}^+)$ remain slightly negative at all Y , most probably due to finite duct aspect ratios.

V. DISCUSSION

The starting point for the present study was the observation that it is hardly possible to fit the free-stream velocity in the ZPG TBL [Eq. (3)] and the centerline velocities in channels [Fig. 8 and Eq. (9)] and pipes [Fig. 4 and Eq. (4)] with a single universal Kármán constant. From standard asymptotic matching principles (see Sec. I), it follows that the κ 's of the external log-regions, which are the overlap layers or common parts of the inner and outer expansions of the three canonical flows, must also be different and related to the different pressure gradients. Indeed, the parameters κ_{ext} and B_{ext} of the three exterior logarithmic overlap layers $U_{\text{cp}}^+ = \kappa_{\text{ext}} \ln(y^+) + B_{\text{ext}}$ extracted in this study and collected in Table I, together with the additive constants C in the log-laws for U_{∞}^+ and U_{CL}^+ , are found to be a monotonically increasing function of the favorable pressure gradient. Furthermore, they closely follow the correlation

$$\kappa_{\text{ext}} B_{\text{ext}} = 1.6 [\exp(0.163 B_{\text{ext}}) - 1], \quad (14)$$

which is virtually identical to Eq. (13) of Nagib and Chauhan [9] based on a wide range of pressure gradient boundary layers. It is worth noting that the positive curvature of the graph $\kappa_{\text{ext}} B_{\text{ext}}$ versus B_{ext} necessarily implies the monotonic increase of κ_{ext} with increasing favorable pressure gradient, which is at odds with the low κ given by Nagib and Chauhan [9] for the channel.

Beyond the correlation Eq. (14), the increase of κ_{ext} relative to its value in ZPG TBL's can now be directly related to the Clauser pressure gradient parameter based on Re_{τ} , $\beta = -\text{Re}_{\tau} (dp^+/dx^+)$ with $p^+ \equiv \hat{p}/(\hat{\rho} \hat{u}_{\tau}^2)$, which is equal to 1 and 2 for channel and pipe flow, respectively. The simple power law

$$\kappa_{\text{ext}} - 0.384 = 0.029 \beta^n, \quad (15)$$

with $n = (1/3)$ provides a good fit for the values of κ_{ext} in Table I. However, the value of $(1/3)$ for the exponent in Eq. (15) needs to be taken “with a grain of salt” as it is based on only two points and the uncertainty of κ_{ext} for the pipe in particular is large. If, for instance, κ_{ext} for the pipe is increased to 0.442, the exponent n in Eq. (15) increases to unity. Interestingly, 0.442 is within the error bars of the original value of 0.436 obtained by Zagarola and Smits [14] in the Superpipe, and of the 0.437 of Fiorini [26] and the latest value of 0.446 obtained by Nagib *et al.* [48] in the new CICLoPE pipe.

Looking for a theoretical underpinning of the observed increase of κ_{ext} with β , one may first consider the integrated momentum balance in inner variables, in the region where the mean velocity profile is logarithmic,

$$-\frac{\beta}{\text{Re}_\tau} y^+ + \frac{1}{\kappa y^+} - \langle uv \rangle^+ = 1. \quad (16)$$

From the balance of the first two terms, one would conclude that the pressure gradient becomes significant beyond a y^+ of order $\mathcal{O}(\text{Re}_\tau/\beta)^{1/2}$ which is not borne out by the data. Figure 5, in particular, clearly excludes $y_{\text{int-ext}}^+ \propto \text{Re}_\tau^{1/2}$. This points to a possible indirect action of the pressure gradient, which modifies the turbulence structures generating the Reynolds stress above $y_{\text{int-ext}}^+$ and causes an adaptation of the logarithmic slope of U^+ to balance the equation.

A more formal argument for the effect of β on turbulent wall-bounded flows has recently been proposed by Luchini [49]. In his paper, Luchini generalizes Millikan’s dimensional matching argument to parallel flows with weak pressure gradients and obtains the modified overlap profile $U_{\text{cp}}^+ = (1/\kappa) \ln(y^+) + 4.48 + A_1 \beta (y^+/\text{Re}_\tau)$ with the parameters $\kappa = 0.392$ and $A_1 = 1$ determined from low Reynolds number DNS without clean log regions [his Eq. (7) with $g \equiv \beta$]. The first observation is that Luchini’s overlap profile actually steepens with increasing β . If one were to locally fit the usual $(1/\kappa) \ln(y^+) + B$ to Luchini’s expression, one would find κ ’s that *decrease* with β , which is clearly contrary to the present findings, i.e., incompatible with the observed increase of centerline κ ’s with β . The problem can be traced back to Luchini’s assertion that his Eq. (6) is the *only* dimensionally correct extension of the original Millikan matching argument to weak pressure gradients. This is because only the wall friction $\widehat{\tau}_{\text{wall}}$ was included in the list of available dimensional quantities to obtain a dimensionally correct Eq. (6), while the overall dimension \widehat{L} of the flow cross-section (pipe radius or channel half height) was excluded without good reason: replacing A_1 in Luchini’s Eq. (6) by $-0.197(\widehat{L}/\widehat{y})$ actually yields, for $\kappa = 0.384$, the present Eq. (15) with $n = 1$.

So, what remains of universality is the buffer layer and an interior log layer with the same (within fitting accuracy) $\kappa_{\text{int}} = 0.384$ and additive constant $B_{\text{int}} = 4.22$ as in the ZPG TBL, as sketched in Fig. 1. However, this region with universal $U^+(y^+)$ has been found to shrink with increasing pressure gradient: While it extends to $y_{\text{int-ext}}^+ \approx 700$ in the channel, its thickness is reduced to ≈ 500 wall units in the pipe (see Table I). Note, however, that in the channel the exterior log-law, i.e., the logarithmic overlap layer, remains “buried” in the wake at all the available H^+ , so that $y_{\text{int-ext}}^+ \approx 700$ can only be a rough estimate. Despite the large uncertainty of these switch-over points, the trend appears rather clear and consistent with an increasing pressure gradient becoming significant in the momentum balance closer and closer to the wall.

The proposed double log-layer structure for wall-bounded flows with weak pressure gradients, specifically pipe and channel flows, resolves the apparent conflict between the log-law parameters extracted from centerline data and those obtained from near-wall velocity profiles, especially from profiles at Reynolds numbers below $\text{Re}_\tau \approx 10^4$, where in the overwhelming majority of experiments and computations the Kármán constant κ is found to be within ± 0.005 of the ZPG TBL value of 0.384.

Considering the observed trend of $y_{\text{int-ext}}^+$ with pressure gradient, one may speculate that the interior logarithmic region will disappear for pressure gradients not much larger than in the pipe. Conversely, one would expect an expansion of the universal interior logarithmic region when reducing the pressure gradient below the channel value. Exploring these ideas experimentally appears exceedingly difficult, but it may be interesting to explore high Reynolds number channel flows with artificially altered friction on one of the walls by high resolution DNS.

ACKNOWLEDGMENTS

I am most grateful to Hassan Nagib for his continuous encouragement and even more so for initiating this research by relating to me his discussion with Don Coles, in which Don asked him why he was bothering to extract κ 's from velocity profiles when it was so much easier and more reliable to do it from free-stream or centerline data. I also thank Marcus Hultmark, MyoungKyu Lee, Gilmar Mompean, Bob Moser, Hassan Nagib, and Mike Schultz for sharing data and Ivan Marusic for the data file corresponding to Fig. 1 in Ref. [11].

APPENDIX A: MODIFIED MUSKER FIT FOR THE INNER PART OF THE ZPG TBL

For convenience, the ‘‘Musker’’ fit for the inner part $U^+(y^+)$ of the ZPG TBL mean velocity profile up to and including the logarithmic overlap layer, as modified by Chauhan *et al.* [18] is reproduced below:

$$U_{\text{inner,ZPG}}^+ = \frac{1}{\kappa} \ln\left(\frac{y^+ + a}{a}\right) - \frac{\gamma^2}{a(4\alpha + a)} \left[(4\alpha - a) \ln\left(\frac{a\sqrt{(y^+ - \alpha)^2 + \beta^2}}{\gamma(y^+ + a)}\right) + \frac{\alpha(4\alpha - 5a)}{\beta} \arctan\left(\frac{\beta y^+}{\alpha^2 + \beta^2 - \alpha y^+}\right) \right] + \frac{1}{2.85} \exp[-\ln^2(y^+/30)], \quad (\text{A1})$$

with $\alpha = (a - 1/\kappa)/2$, $\beta = \sqrt{2a\alpha - \alpha^2}$ and $\gamma = \sqrt{\alpha^2 + \beta^2}$. With $\kappa = 0.384$ and $a = 10.3538$, the common part of inner and outer expansions is given by Eq. (2).

APPENDIX B: AN ATTEMPT TO FIT THE SUPERPIPE DATA WITH THE ZPG TBL OVERLAP LAYER

As discussed in Secs. I and III, the asymptotic matching argument for equal κ 's in Eq. (4) for the pipe centerline velocity and in the overlap layer adjacent to the wake hinges on the assumption that the outer expansion can be limited to two terms of order $\mathcal{O}(\ln R^+)$ and $\mathcal{O}(1)$. This assumption is strongly supported by the following failed attempt to develop an outer expansion, which has the same common part, Eq. (2), as the ZPG TBL.

Starting again with the centerline, the fit proposed by Monkewitz and Nagib [13],

$$U_{\text{CL,alt}}^+ = \frac{1}{0.384} \ln(R^+) + 2.35 + \frac{22}{\ln(R^+)}, \quad (\text{B1})$$

is seen in Fig. 10 to be as good as Eq. (4) over the R^+ -range of available data.

A general outer fit reducing to Eq. (B1) on the centerline is

$$U_{\text{alt outer,P}}^+ = \frac{1}{0.384} \ln\left\{\frac{5.05}{0.5\pi} R^+ \sin\left(\frac{\pi Y}{2}\right)\right\} + f(Y) + \frac{g(Y)}{\ln(R^+)}, \quad (\text{B2})$$

implying that $f(1) = -0.69$ and $g(1) = 22$. If the fit by Eq. (B2) is to be universal, f and g must be universal functions of Y . They can be determined from pairs of experimental profiles $U_{\text{p}}^+ - U_{\text{inner,ZPG}}^+$ in Fig. 5. The results for f and g , obtained by pairing the seven lowest and the six highest R^+ with

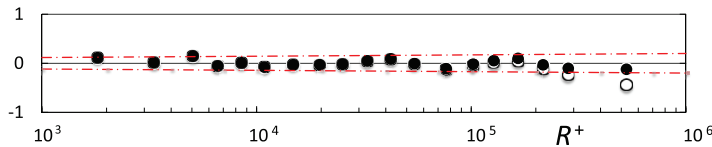


FIG. 10. Superpipe Pitot centerline velocities minus $U_{\text{CL,alt}}^+$ [Eq. (B1)] versus R^+ . ●, ○, same as in Fig. 4. - - - (red), $\pm 0.5\%$ of $U_{\text{CL,alt}}^+$.

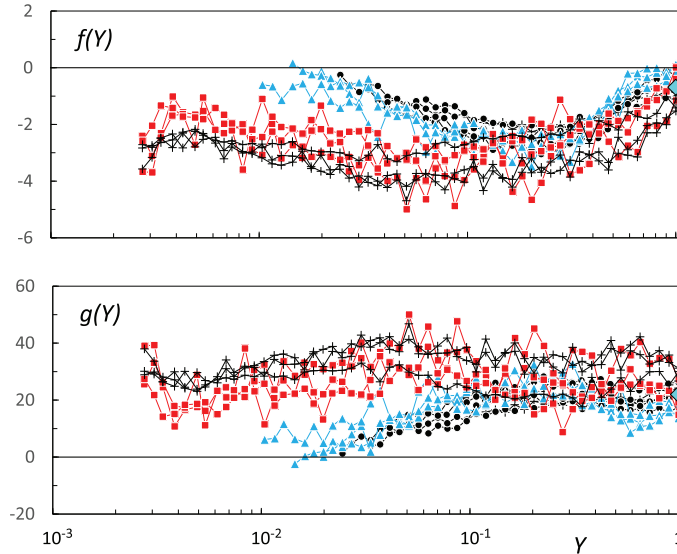


FIG. 11. $f(Y)$ and $g(Y)$ of the alternate outer fit Eq. (B2) obtained by pairing the seven lowest and the six highest R^+ of Fig. 5 with the reference 11th profile ($R^+ = 4.21 \times 10^4$). \blacklozenge , $f(1) = -0.69$ and $g(1) = 22$ required to match the centerline fit [Eq. (B1)]. Other symbols as in Fig. 5.

the 11th profile for $R^+ = 4.21 \times 10^4$ as reference and using only data for $y^+ > 200$, are seen in Fig. 11 to be rather noisy. Nevertheless, the figure clearly shows that the data are not compatible with universal $f(Y)$ and $g(Y)$ in Eq. (B2). The difference between the $f(Y)$ obtained from low and high Reynolds number profiles is particularly marked in the region $Y \lesssim 0.1$, i.e., in the region of the exterior log region of Fig. 5 with $\kappa = 0.42$, where the difference between $f(Y)$ from low and high Reynolds number pairs reaches 2, whereas the new fit in Sec. III fits the data within ± 0.2 , as seen in Fig. 7(b). Of course, one could try gauge functions other than $(1/\ln R^+)$ in Eqs. (B1) and (B2), but it is clear that no corrective term in the outer expansion with a gauge function $\ll 1$ can properly describe a function of the inner variable alone, such as the deviation Eq. (5) from the ZPG TBL log-law.

-
- [1] L. Prandtl, Bericht über Untersuchungen zur ausgebildeten Turbulenz, *ZAMM* **5**, 136 (1925).
 - [2] Th. von Kármán, Turbulence and skin friction, *J. Aero. Sci.* **1**, 1 (1934).
 - [3] A. Segalini, R. Örlü, and P. H. Alfredsson, Uncertainty analysis of the von Kármán constant, *Exp. Fluids* **54**, 1460 (2013).
 - [4] F. H. Clauser, The turbulent boundary layer, *Adv. Mech.* **4**, 1 (1956).
 - [5] T. Wei, R. Schmidt, and P. McMurtry, Comment on the Clauser chart method for determining the friction velocity, *Exp. Fluids* **38**, 695 (2005).
 - [6] L. H. Tanner and L. G. Blows, A study of the motion of oil films on surfaces in air flow, with application to the measurement of skin friction, *J. Phys. E: Sci. Instruments* **9**, 194 (1976).
 - [7] H. H. Fernholz, G. Janke, M. Schober, P. M. Wagner, and D. Warnack, New developments and applications of skin-friction measuring techniques, *Meas. Sci. Technol.* **7**, 1396 (1996).
 - [8] M. V. Zagarola and A. J. Smits, Scaling of the Mean Velocity Profile for Turbulent Pipe Flow, *Phys. Rev. Lett.* **78**, 239 (1997).

- [9] H. M. Nagib and K. A. Chauhan, Variations of von Kármán coefficient in canonical flows, *Phys. Fluids* **20**, 101518 (2008).
- [10] R. Örlü, J. H. M. Fransson, and P. H. Alfredsson, On near wall measurements of wall bounded flows — The necessity of an accurate determination of the wall position, *Progr. Aero. Sci.* **46**, 353 (2010).
- [11] I. Marusic, J. P. Monty, M. Hultmark, and A. J. Smits, On the logarithmic region in wall turbulence, *J. Fluid Mech. Rapids* **716**, R3 (2013).
- [12] D. E. Coles, The law of the wake in the turbulent boundary layer, *J. Fluid Mech.* **1**, 191 (1956).
- [13] P. A. Monkewitz and H. M. Nagib, How comparable are the three “canonical” turbulent flows? in *Proceedings of ICTAM 2016, Vol. 2, Montreal, Canada*, edited by J. M. Floryan (IUTAM, 2017), pp. 484.
- [14] M. V. Zagarola and A. J. Smits, Mean-flow scaling of turbulent pipe flow, *J. Fluid Mech.* **373**, 33 (1998).
- [15] B. J. McKeon, J. Li, W. Jiang, J. F. Morrison, and A. J. Smits, Further observations on the mean velocity distribution in fully developed pipe flow, *J. Fluid Mech.* **501**, 135 (2004).
- [16] S. C. C. Bailey, M. Hultmark, J. P. Monty, P. H. Alfredsson, M. S. Chong, R. D. Duncan, J. H. M. Fransson, N. Hutchins, I. Marusic, B. J. McKeon, H. M. Nagib, R. Örlü, A. Segalini, A. J. Smits, and R. Vinuesa, Obtaining accurate mean velocity measurements in high Reynolds number turbulent boundary layers using Pitot tubes, *J. Fluid Mech.* **715**, 642 (2013).
- [17] V. Kulandaivelu, Evolution and structure of zero pressure gradient turbulent boundary layer, Ph.D. thesis, University of Melbourne (2011).
- [18] K. A. Chauhan, P. A. Monkewitz, and H. M. Nagib, Criteria for assessing experiments in zero pressure gradient boundary layers, *Fluid Dynam. Res.* **41**, 021404 (2009).
- [19] J. C. Rotta, Turbulent boundary layers in incompressible flow, *Prog. Aero. Sci.* **2**, 1 (1962).
- [20] P. A. Monkewitz, K. A. Chauhan, and H. M. Nagib, Self-consistent high-Reynolds-number asymptotics for zero-pressure-gradient turbulent boundary layers, *Phys. Fluids* **19**, 115101 (2007).
- [21] I. Marusic, B. J. McKeon, P. A. Monkewitz, H. M. Nagib, A. J. Smits, and K. R. Sreenivasan, Wall-bounded turbulent flows at high Reynolds numbers: Recent advances and key issues, *Phys. Fluids* **22**, 065103 (2010).
- [22] A. Segalini, J.-D. Ruedi, and P. A. Monkewitz, Systematic errors of skin-friction measurements by oil-film interferometry, *J. Fluid Mech.* **773**, 298 (2015).
- [23] J. Nikuradse, Gesetzmässigkeiten der turbulenten Strömung in glatten Röhren, VDI Forschungsheft (English translation: NASA TT F-10, 359) **365**, 1 (1932).
- [24] N. Furuichi, Y. Terao, Y. Wada, and Y. Tsuji, Friction factor and mean velocity profile for pipe flow at high Reynolds numbers, *Phys. Fluids* **27**, 095108 (2015).
- [25] A. Talamelli, F. Persiani, J. H. M. Fransson, P. H. Alfredsson, A. V. Johansson, H. M. Nagib, J.-D. Ruedi, K. R. Sreenivasan, and P. A. Monkewitz, CICLoPE—A response to the need for high Reynolds number experiments, *Fluid Dynam. Res.* **41**, 021407 (2009).
- [26] T. Fiorini, Turbulent Pipe Flow—High Resolution Measurements in CICLoPE, Ph.D. thesis, University of Bologna (2017).
- [27] R. Örlü, T. Fiorini, A. Segalini, G. Bellani, A. Talamelli, P. H. Alfredsson, Reynolds stress scaling in pipe flow turbulence—First results from CICLoPE, *Phil. Trans. R. Soc. A* **375**, 20160187 (2016).
- [28] E. S. Zanoun, F. Durst, O. Bayoumy, and A. Al-Salaymeh, Wall skin friction and mean velocity profiles of fully developed turbulent pipe flows, *Exp. Thermal Fluid Sci.* **32**, 249 (2007).
- [29] B. J. McKeon and A. J. Smits, Static pressure correction in high Reynolds number fully developed turbulent pipe flow, *Meas. Sci. Tech.* **13**, 1608 (2002).
- [30] B. J. McKeon, J. D. Li, W. Jiang, J. F. Morrison, and A. J. Smits, Pitot probe corrections in fully-developed turbulent pipe flow, *Meas. Sci. Tech.* **14**, 1449 (2003).
- [31] R. Vinuesa, R. D. Duncan, and H. M. Nagib, Alternative interpretation of the superpipe data and motivation for ciclope: The effect of decreasing viscous length scale, *Eur. J. Mech. B Fluids* **58**, 109 (2016).
- [32] J. J. Allen, M. A. Shockling, and A. J. Smits, Evaluation of a universal transitional resistance diagram for pipes with honed surfaces, *Phys. Fluids* **17**, 121702 (2005).
- [33] S. C. C. Bailey, M. Vallikivi, M. Hultmark, and A. J. Smits, Estimating the value of von Kármán’s constant in turbulent pipe flow, *J. Fluid Mech.* **749**, 79 (2014).

- [34] M. Hultmark, M. Vallikivi, S. C. C. Bailey, and A. J. Smits, Turbulent Pipe Flow at Extreme Reynolds Numbers, *Phys. Rev. Lett.* **108**, 094501 (2012).
- [35] A. E. Perry and C. J. Abell, Asymptotic similarity of turbulence structures in smooth- and rough-walled pipes, *J. Fluid Mech.* **79**, 785 (1977).
- [36] J. P. Monty, Developments in smooth wall turbulent duct flows, Ph.D. thesis, University of Melbourne (2005).
- [37] J. Klewicki, J. Philip, I. Marusic, K. Chauhan, and C. Morrill-Winter, Self-similarity in the inertial region of wall turbulence, *Phys. Rev. E* **90**, 063015 (2014).
- [38] P. A. Monkewitz and H. M. Nagib, Large Reynolds number asymptotics of the stream-wise normal stress in ZPG turbulent boundary layers, *J. Fluid Mech.* **783**, 474 (2015).
- [39] R. Vinuesa and H. M. Nagib, Enhancing the accuracy of measurement techniques in high reynolds number turbulent boundary layers for more representative comparison to their canonical representations, *Eur. J. Mech. B Fluids* **55**, Part 2, 300 (2016).
- [40] R. Vinuesa, E. Bartrons, D. Chiu, K. M. Dressler, J.-D. Rüedi, Y. Suzuki, and H. M. Nagib, New insight into flow development and two dimensionality of turbulent channel flows, *Exp. Fluids* **55**, 1759 (2014).
- [41] R. Vinuesa, A. Noorani, A. Lozano-Durán, G. K. El Khoury, P. Schlatter, P. F. Fischer, and H. M. Nagib, Aspect ratio effects in turbulent duct flows studied through direct numerical simulation, *J. Turbul.* **15**, 677 (2014).
- [42] S. Hoyas and J. Jiménez, Scaling of the velocity fluctuations in turbulent channels up to $Re_\tau = 2003$, *Phys. Fluids* **18**, 011702 (2006).
- [43] A. Lozano-Durán and J. Jiménez, Effect of the computational domain on direct numerical simulations of turbulent channels up to $Re_\tau = 4200$, *Phys. Fluids* **26**, 011702 (2014).
- [44] M. Lee and R. D. Moser, Direct numerical simulation of turbulent channel flow up to $Re_\tau = 5200$, *J. Fluid Mech.* **774**, 395 (2015).
- [45] L. Thais, G. Mompean, and T. Gatski, Spectral analysis of turbulent viscoelastic and newtonian channel flows, *J. Non-Newtonian Fluid Mech.* **200**, 165 (2013).
- [46] E. S. Zanoun, F. Durst, and H. M. Nagib, Evaluating the law of the wall in two-dimensional fully developed turbulent channel flows, *Phys. Fluids* **15**, 3079 (2003).
- [47] M. P. Schultz and K. A. Flack, Reynolds number scaling of turbulent channel flow, *Phys. Fluids* **25**, 025104 (2013).
- [48] H. M. Nagib, P. A. Monkewitz, L. Moscotelli, T. Fiorini, G. Bellani, X. Zheng, and A. Talamelli, Centerline Kármán “constant” revisited and contrasted to log-layer Kármán constant at CICLoPE, in *Proceedings of TSFP10, Chicago, IL*, edited by H. M. Nagib and A. J. Smits (2017).
- [49] Paolo Luchini, Universality of the Turbulent Velocity Profile, *Phys. Rev. Lett.* **118**, 224501 (2017).